



Green Synthesis, Characterization, and Photocatalytic Activity of Zinc Oxide Nanoparticles on Photodegradation of Naphthol Blue Black Dye

Jesisca Silver¹, Surya Lubis^{1,*}, Muliadi Ramli¹

¹ Department of Chemistry, Faculty of Mathematics and Natural Sciences, Universitas Syiah Kuala, Darussalam 23111, Banda Aceh, Indonesia

* Corresponding author: suryalubis@usk.ac.id

<https://doi.org/10.14710/jksa.26.9.363-371>

Article Info

Article history:

Received: 22nd September 2023

Revised: 29th November 2023

Accepted: 30th November 2023

Online: 30th November 2023

Keywords:

Zinc oxide; nanoparticles; red dragon fruit; naphthol blue black

Abstract

Zinc oxide (ZnO) nanoparticles have been successfully synthesized using water extract of red dragon fruit (*Hylocereus polyrhizus*) stem with zinc acetate dihydrate as a precursor of ZnO. Chemical compounds contained in the red dragon fruit stem extract, such as phenolics, terpenoids, and steroids, acted as reducing agents, stabilizers, and capping agents. The phase structure, crystallite size, functional groups, shape, and morphology of ZnO nanoparticles were determined by X-ray diffraction (XRD), Fourier Transform infrared (FTIR) Spectroscopy, and Scanning Electron Microscopy–Energy Dispersive X-ray (SEM–EDX). The XRD pattern confirmed the crystallinity of synthesized zinc oxide was in the zincite (ZnO) phase with an average crystallite size of 79.09 nm. Spectroscopy FTIR analysis showed that the synthesized ZnO nanoparticles had characteristics similar to the ZnO standard/commercial. SEM–EDX analysis revealed that the synthesized ZnO nanoparticles were spherical, evenly distributed, and homogeneous particle size. The photocatalytic activity of synthesized ZnO nanoparticles was evaluated on the photodegradation of naphthol blue black (NBB) dye. The results showed that the synthesized ZnO nanoparticles have high photocatalytic activity that can degrade NBB dye up to 98.82%. This high photocatalytic activity was obtained at operating parameter conditions with the initial pH of NBB at 2, the dosage of ZnO nanoparticles at 250 mg, and the initial dye concentration at 10 ppm.

1. Introduction

Heterogeneous photocatalytic using photocatalyst materials with low cost and high efficiency was considered one of the effective methods for water remediation. Zinc oxide (ZnO) is one of the most widely used photocatalysts because of its high photocatalytic activity, high photosensitivity and stability, low cost, and simple manufacturing process [1]. Recently, many researchers have focused on synthesizing and applying nanocatalyst materials, including ZnO nanoparticles. Nanomaterials, materials with small sizes in the range of 1–100 nm and a higher specific surface area appropriate for catalysis, are synthesized with controllable sizes and morphologies affecting the photocatalytic activity. Physical and chemical synthesis methods have been developed for manufacturing ZnO nanoparticles, such as

co-precipitation [2], sol-gel [3], hydrothermal [4], ball milling [5], microwave assistance [6], and green synthesis using plant extracts [7, 8]. Green synthesis is the best route for manufacturing ZnO nanoparticles because it can produce nanoparticles with small size and large surface area and protect the environment from hazardous chemicals.

Zinc oxide (ZnO) is a non-toxic inorganic semiconductor used as a photocatalyst. Zinc oxide has three crystalline forms: wurtzite, zincblende, and rock salt. The ZnO compound has a band gap energy (band gap) of 3.37 eV at room temperature and a bond energy of 60 MeV [9]. ZnO nanoparticles have different chemical, physical, and biological properties from single atoms or bulky molecules. ZnO nanoparticles are widely applied in various fields: biomedical, agriculture, food, textile,

industry, energy, and others. The large band gap, high surface area to volume ratio, and crystallinity of ZnO nanoparticles contributed to the photocatalytic efficiency [10].

The synthesis of ZnO nanoparticles using plant extracts is very interesting because it is simple, easy to handle, cost-effective, and does not use harmful chemicals. Hence, it is safe for the environment. Different phytochemicals contained in plant extracts and precursors of zinc salt determine the final morphology and size of the ZnO nanoparticle. The chemical compounds in plant extracts act as a reducing agent, capping agent, and stabilizer. A plant's roots, stems, leaves, fruits, seeds, and leaves have been utilized to synthesize ZnO nanoparticles [10]. The source of plant extracts influences the characteristics of the synthesized ZnO nanoparticles [11] because different extracts contain different phytochemicals and concentrations [12].

The green synthesis of ZnO nanoparticles using various parts of plants, including stems of *Euphorbia tirucalli* (pencil cactus) [7], which was found to be very effective in degrading 85.3% of rhodamine B dye for 210 minutes irradiation, and lychee peel extract that could effectively remove 98% of congo red dye from wastewater within 2 hours of contact time [13] have been reported. Furthermore, preparation of ZnO nanoparticles using extract of *Alchemilla vulgaris* leaves which can degrade 75% of rhodamine B dye after irradiating for 2 hours [14], extract of dragon fruit peel (*Hylocereus polyrhizus* [15] that has 95% degradation efficiency toward methylene blue dye after irradiating under sunlight for 2 hours, and white dragon fruit (*Hylocereus undatus*) peel that could be used as a potent antimicrobial agent [16], also have been reported in literature.

Dragon fruit plants belong to the family Cactaceae have been widely cultivated in Indonesia. The stems of dragon fruit have never been used and are only disposed of as waste. Therefore, in this study, the biosynthesis of ZnO nanoparticles will be carried out using red dragon fruit (*Hylocereus polyrhizus*) stem extract. This research aims to biosynthesize ZnO nanoparticles and investigate their photocatalytic activity on the photodegradation of NBB dye. Naphthol blue black (Figure 1) is an azo group dye with two azo groups ($-N=N-$) with the molecular formula of $C_{22}H_{14}N_6Na_2O_6S_2$. This dye is often used in the textile industry for dyeing batik, silk, wool, nylon, and textile printing. NBB dyes are known as acid synthesis dyes, are blue-black in color, and are stable at room temperature and pressure. In addition, this dye can pollute the environment because of its non-biodegradable, carcinogenic, and even mutagenic properties [17, 18].

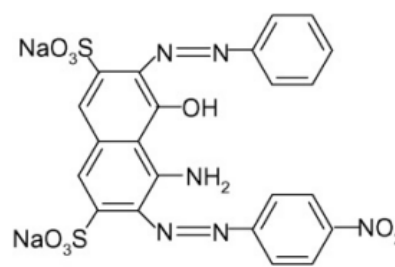


Figure 1. Molecular structure of naphthol blue black

2. Experimental

2.1. Materials

$Zn(CH_3CO_2)_2 \cdot 2H_2O$, HCl, and naphthol blue black (NBB) were purchased from Merck and used without further purification. Fresh red dragon fruit stems were taken from a dragon fruit plantation in Banda Aceh, Indonesia.

2.2. Preparation of Red Dragon Fruit Stem Extract

The preparation of red dragon fruit water extract was carried out based on the previous report, which used the stem of pencil cactus [7]. Fresh red dragon fruit stems were washed thoroughly with distilled water and cut into small pieces. The red dragon fruit stem extract was prepared by taking 100 g, putting it into 400 mL of distilled water, and then boiling it at $80^\circ C$ for 1 hour. After cooling to room temperature, the mixture was filtered using filter paper, and the filtrate obtained was collected and used for phytochemical tests and synthesis of ZnO nanoparticles.

2.3. Phytochemical Test of Red Dragon Fruit Stem Extract

Phytochemical tests were conducted to determine secondary metabolites in the red dragon fruit stem water extract, including alkaloids, steroids, terpenoids, saponins, flavonoids, and phenolic compounds. The phytochemical tests were conducted based on the standard method. The results were designed as (+) for the presence and (-) for the absence of secondary metabolites. The presence of alkaloids was determined by Dragendorff's test (by the formation of an orange-red color precipitate), Mayer's test (by the appearance of a cream-colored precipitate), and Wagner's test (by the formation of a brown-colored precipitate). The Liebermann-Burchard test was used to determine the presence of steroids (by the formation of green or blue color) and terpenoids (by the formation of red color).

A test for the existence of saponins was performed by adding distilled water to the extract and shaking. The formation of foam, which lasted 30 minutes, indicated the presence of saponins. Magnesium powder and hydrochloric acid solution were used to evaluate the presence of flavonoids. The formation of red or purple color indicated the (+) test. The phenolic compounds were detected by dropping $FeCl_3$ solution into the extract, and the formation of a black or dark blue color showed the presence of phenolics [19, 20].

2.4. Green synthesis of Zinc Oxide (ZnO) Nanoparticles

The green synthesis of ZnO nanoparticles using water extract from red dragon fruit stem was conducted based on the previously reported with a slight modification [21], and the process is represented in Figure 2. About 50 mL of red dragon fruit stem extract was put into a beaker and was heated until the temperature reached 60°C. Five g of Zn(CH₃CO₂)₂·2H₂O was added to the dragon fruit stem extract, and the mixture was continuously heated to a temperature of 60–80°C. The color of the mixture turned from pale yellow to deep yellow, and further heating resulted in a yellow paste. The yellow paste was dried at 100°C for 12 hours to produce a greenish-yellow solid. The solid was ground and calcined at 800°C for 5 hours. The resultant white powder was used to characterize and evaluate its photocatalytic activity.

2.5. Characterization of ZnO Nanoparticles

The crystalline phase and crystallite size of synthesized ZnO nanoparticles were investigated using a Shimadzu X-ray diffractometer (XD-7000) equipped with Cu-K α radiation source ($\lambda = 1.54056 \text{ \AA}$) that operating at 40 kV and 30 mA. The scan rate was 5° min⁻¹ with Bragg angle 2 θ was ranged from 10 to 80°. The crystallite sizes (D) of ZnO nanoparticles were determined from the broadening of diffraction peaks according to Scherrer’s formula (Equation (1) [8], where k is the shape factor (the value is 0.9), λ is the X-ray wavelength, β is the full width at half maximum (FWHM) measured in radians of the reflection peak and θ is the Bragg’s angle.

$$D = \left(\frac{k \times \lambda}{\beta \times \cos \theta} \right) \tag{1}$$

FTIR spectrophotometer (Shimadzu) was used to determine the functional groups in ZnO nanoparticles in the range wavenumber 400–4000 cm⁻¹. The morphologies of the sample surface were examined by a Scanning Electron Microscope (SEM) (JEOL JSM6510LV) operated at an acceleration voltage of 15 kV, while the composition of elements was analyzed using EDX. A Shimadzu UV-2450 UV/Vis spectrophotometer was employed to study absorption and bandgap at the 200 to 800 nm wavelength range.

2.6. Photocatalytic Experiment

The photocatalytic degradation of NBB dye was studied under ultraviolet (using a 6-W UV lamp, $\lambda = 365 \text{ nm}$). The entire arrangement was placed in a box to avoid the passage of other light from outside. The pH of the NBB dye solution was measured on the HI98107 pHep pH tester and was adjusted to pH 2. Typically, 250 mg of ZnO nanoparticles was added to 25 mL of 10 ppm NBB dye solution on the Pyrex glass vessel. The mixture was placed about $\pm 10 \text{ cm}$ from the UV lamp. The experiments were carried out for 300 minutes, consisting of 30 minutes in darkness and 90, 180, and 270 minutes under UV light irradiation. After the time interval was reached, the suspensions were centrifuged for 10–15 minutes to remove the photocatalyst completely. The concentrations of NBB dye were determined using a UV-Vis spectrophotometer (Shimadzu UV mini 1240 spectrophotometer) at λ_{max} of 617 nm. The percent removal of NBB dye was estimated using Equation (2). The experiments were also performed using ZnO nanoparticles and 25 mL of NBB dye solution without UV light (dark condition).

$$\%D = (C_0 - C_t) / C_0 \times 100\% \tag{2}$$

where C₀ and C_t presented the initial and final dye concentration (ppm) [22].

3. Results and Discussion

3.1. Phytochemical Test of Red Dragons Fruit Stems (Hylocereus polyrhizus) Extract

The phytochemicals present in the red dragon extract are essential for biosynthesizing ZnO nanoparticles. The secondary metabolites in red dragon fruit stem extract reduce metal ions to metal nanoparticles, act as a capping/stabilizer agent, and control the size of synthesized nanoparticles [23, 24]. The results of the phytochemical test (Table 1) showed that water extract of the red dragon fruit stem contained steroids, terpenoids, and phenolics, while alkaloids, saponins, and flavonoids were not found. Based on this result, the phytochemicals in red dragon fruit stem extract have the potential as a bio-reductor and capping/stabilizer agent.

Table 1. Phytochemical test results of red dragon fruit stem (Hylocereus polyrhizus) water extract

Phytochemical Test	Observation	Result
Alkaloids	Wagner	no brown color precipitate
	Mayer	no white or orange color precipitate
	Dragendorff	no orange or red color precipitate
Steroid	Lieberman Burchard	yellow color
Terpenoid	Lieberman Burchard	red color
Saponin	Distilled water and shaken process	no foam
Flavonoid	Mg and HCl	no pink color
Phenolic	FeCl ₃	Blackish green color

3.2. Green Synthesis of ZnO Nanoparticles by Using Red Dragons Fruit Stems (*Hylocereus polyrhizus*) Extract

Synthesis of ZnO nanoparticles was carried out using red dragon fruit stem water extract as a bio-reductor and capping/stabilizer agent with zinc acetate dihydrate as a ZnO precursor. Table 1 shows terpenoids acting as a reduction agent for Zn²⁺ ions, while phenolics are responsible for the capping/stabilizer agent for reduced nanoparticles. In addition, phenolic compounds also play a role in reducing and capping zinc ions [21, 25].

The secondary metabolite, which contains the -OH group, acts as a bio-reductor, reducing Zn²⁺ to Zn⁰. The secondary metabolite in plant extract also acts as a stabilizer/capping agent to inhibit the development of nanoparticle size and prevent the accumulation of ZnO nanoparticles. The other process is the formation of hydroxyl chelation from phytochemical compounds to ion Zn²⁺ ion, which leads to the formation of an intermediate product, zinc hydroxide (Zn(OH)₂), through hydrolysis. The calcination process at high temperatures can cause Zn⁰ to be oxidized to form zinc oxide (ZnO). In addition, the calcination process can also decompose or oxidize Zn-secondary metabolite chelate compounds and Zn(OH)₂ to ZnO [21, 26].

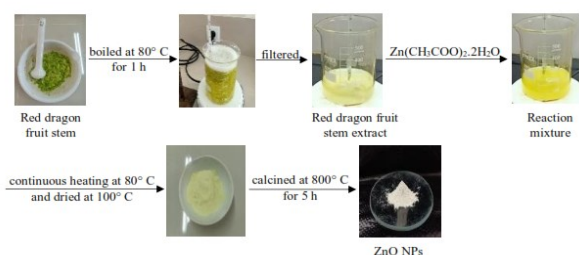


Figure 2. ZnO nanoparticle biosynthesis using red dragon fruit stem extract

3.3. Characterization of Materials

3.3.1. X-ray Diffraction Analysis

The XRD pattern in Figure 3 shows that synthesized zinc oxide nanoparticles using red dragon fruit stem extracts have sharp and narrow diffraction, indicating high crystallinity, small size, and purity. The ZnO nanoparticles have peaks in the diffraction angle at 2θ: 31.75°, 34.44°, 36.25°, 47.57°, 56.56°, 62.90°, 66.33°, 69.04°, 72.58°, 76.94°, 77.09°, and 81.50° that proved the formation of zincite phase ZnO with a hexagonal structure. These results are confirmed regarding the COD database [96–900–4179]. The XRD patterns obtained in this study were also similar to XRD patterns obtained for biologically synthesized ZnO nanoparticles reported in the literature using thyme plant leaf extract [23], *Eucalyptus globulus* Labill. leaf extract [24], and *Tilia Tomentosa* (Ihlamur) [27]. The diffraction pattern of ZnO nanoparticles in Figure 3 also indicated there was no peak at 2θ: 32° caused by Zn(OH)₂, which was formed as one of the resultant reduction processes of Zn²⁺ salt in the red dragon fruit stem water extract [21]. These indicated that the calcination process at 800°C can completely convert Zn(OH)₂ into ZnO.

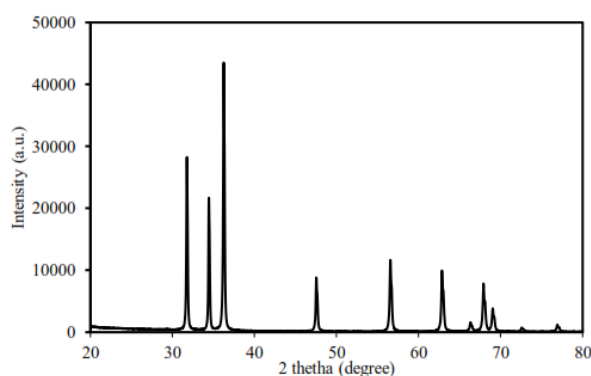


Figure 3. XRD pattern of ZnO nanoparticles

Table 1. The ZnO nanoparticles crystallite size calculation uses the Scherrer formula based on data from Figure 3

Peak number	Planes	2 theta (°)	FWHM	Size (nm)
1	100	31.759	0.101	80.910
2	002	34.440	0.103	79.896
3	101	36.250	0.112	73.846
Average size				79.096

The average crystallite size of ZnO nanoparticles was calculated based on data of FWHM at the three main peaks at 2θ: 31.75°, 34.44°, and 36.25° and it was found to be 79.09 nm, which was confirmed the nanosize of ZnO (Table 1). A similar crystallite size of ZnO was obtained from the biosynthesis using *Mentha longifolia* L. Leaves [28] but larger than that of using thyme plant leaf extract [23], *Eucalyptus globulus* Labill. leaf extract [24], and *Tilia Tomentosa* (Ihlamur) [27]. This difference may occur due to the differences in the secondary metabolite contained as well as differences in calcination temperature.

3.3.2. The Fourier Transform Infrared Spectroscopy Analysis

FTIR spectroscopy analysis was carried out to identify the functional groups in synthesized ZnO nanoparticles. The FTIR spectra of synthesized ZnO nanoparticles and commercial ZnO are shown in Figure 4. It can be seen that the FTIR spectra of synthesized ZnO nanoparticles are almost the same as commercial ZnO. The broad absorption peak at 3454 cm⁻¹ is due to the O-H stretching vibration of the hydroxyl group from the water adsorbed [10], and the other peak at 1624 cm⁻¹ is the H-O-H bending vibration [29]. As previously reported in the literature, the absorption peaks at 437 cm⁻¹ and 511 cm⁻¹ belong to Zn-O stretching vibration [10, 30, 31]. The absorption peak at 1445 cm⁻¹ was attributed to C=O vibration, while the peak at 2341 cm⁻¹ indicated the symmetric COO⁻ stretching vibration modes of the acetate group [31, 32] or because of the presence of CO₂ molecules in the environment [33].

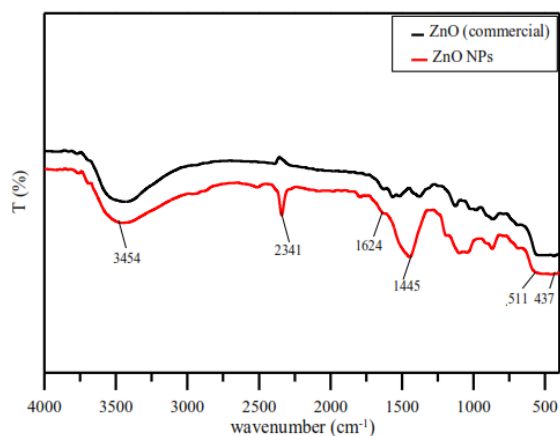


Figure 4. The FTIR spectra of synthesized ZnO nanoparticles and commercial ZnO

3.3.3. Scanning Electron Microscopy–Energy Dispersive X-ray

The surface morphology and elemental composition of synthesized ZnO nanoparticles were investigated employing SEM and EDX. The results of SEM analysis (Figure 5a) showed that ZnO nanoparticles were spherical, well dispersed, and homogeneous particle sizes. The distribution of ZnO nanoparticles occurs evenly and shows only a small amount of agglomeration (Figure 5). The generated ZnO NPs occasionally exhibited significant aggregation formation, which is characteristic of green synthesis nanoparticles. This is because biosynthetic NPs have a larger surface area, and their long-lasting affinities lead to their agglomeration or aggregation [23, 24]. This is a characteristic of an excellent photocatalyst to degrade pollutants such as dyes and other organic compounds.

The EDX spectra of ZnO nanoparticles in Figure 5b reveal the presence of Zn and O without any other element. The EDX spectra displayed three peaks for Zn at 1.0 keV, 8.7 keV, and 9.6 keV, while a single peak at 0.5 keV corresponded to oxygen [15, 23]. The atomic percentages of zinc and oxygen were 55.8% and 45.2%, respectively, while the weight percentages of zinc and oxygen were 83.8% and 16.2%, respectively. The atomic ratio of Zn and O was almost 50:50, which matches the theoretical values [14, 27]. The weight percentage of Zn and O, which was obtained in this study, is close to the bulk ZnO weight percentage (80 for Zn and 20 for O) [30, 34]. The EDX mapping of Zn and oxygen is represented in Figure 6.

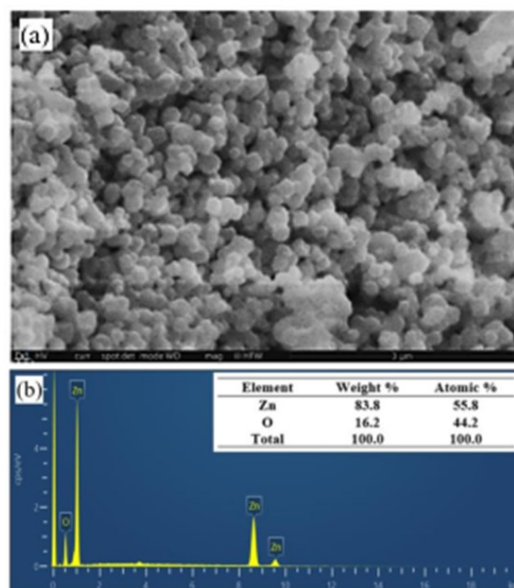


Figure 5. (a) SEM images and (b) EDX spectra of ZnO nanoparticles

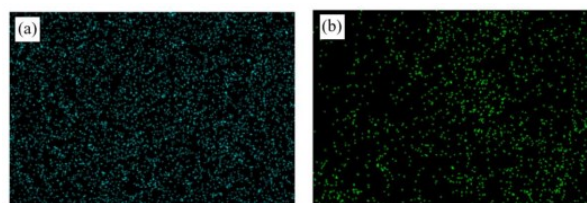


Figure 6. EDX mapping images of (a) Zinc and (b) Oxygen

3.3.4. UV–Vis Diffuse Reflectance Spectroscopy

The optical absorption properties of the prepared ZnO nanoparticles were measured using UV–Vis diffuse reflectance spectroscopy (UV–DRS) at 200–800 nm wavelength (Figure 7a). The bandgap energy of synthesized ZnO nanoparticles was calculated based on the numerical derivative of the optical absorption coefficient using Tauc’s plot between the optical absorption coefficient (α), the photon energy ($h\nu$), the constant (A), and the direct band-gap energy (E_g) (Figure 7b). The band-gap energy was found to be 3.22 eV, almost similar to those reported in the literature for the green synthesis of ZnO nanoparticles [33].

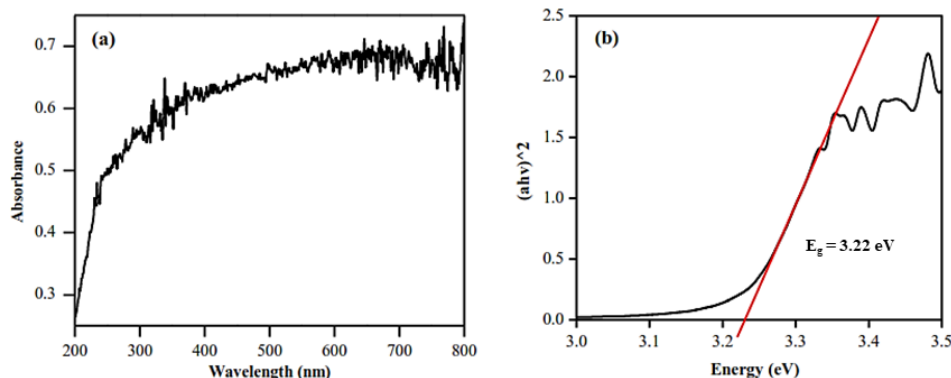


Figure 7 (a) UV–Vis diffuse reflectance (DRS) spectra and (b) Tauc plot of green synthesized ZnO nanoparticles

3.4. Photocatalytic Activity of Synthesized ZnO Nanoparticles

3.4.1. Effect of Irradiation Time on the Photodegradation of NBB Dye

The effect of irradiation time on the photodegradation of NBB dye using ZnO nanoparticles was investigated by monitoring the percent removal of NBB dye at different periods in the presence of UV light. The experiments were conducted at an initial concentration of NBB solution of 10 ppm, the initial pH of NBB solution was 2, and the photocatalyst dosage was 250 mg. Figure 8 shows the absorbance curves corresponding to the decrease in NBB concentration over time. The photodegradation efficiency was calculated using Equation 2. Two significant peaks at 319 and 617 nm are observed that are characteristic of the aromatic structure and the azo groups of NBB [35]. It is observed that both the absorption peaks decrease with the increase of the irradiation time. During the adsorption-desorption process for 30 minutes (without UV irradiation), the absorption peaks were slightly reduced and could only absorb 29.6% of NBB dye.

After irradiation for 90 minutes, the absorption peaks of NBB remain detectable. However, the absorbance value of NBB was significantly reduced after 180 minutes and gave a maximum photodegradation activity of ZnO nanoparticles after irradiation for 270 minutes with the percent removal of NBB at 98.82%. It confirms that the photocatalytic efficacy of ZnO nanoparticles is highly dependent on the irradiation duration. This dependency arises from the increased excitation of electrons from the valence band to the conduction band of ZnO nanoparticles with prolonged irradiation. Consequently, more active species are generated, including hydroxyl radicals ($\cdot\text{OH}$) and superoxide ion radicals ($\text{O}_2^{\cdot-}$). These active species play a pivotal role in the degradation of NBB dye.

The mechanism of photodegradation of NBB dye over ZnO nanoparticles can be explained as follows: the photocatalytic reaction begins when the photon energy from ultraviolet light reaches the surface of ZnO nanoparticles, transferring electrons from the filled valence band to the empty conduction band. The photogenerated electrons and holes can react with NBB molecules, causing the degradation of NBB dye. It is also possible that the presence of photogenerated electrons and holes leads to the formation of superoxide ions ($\text{O}_2^{\cdot-}$) and hydroxyl radicals ($\cdot\text{OH}$). It has been reported that hydroxyl radical is a powerful oxidant for the degradation of many organic compounds [1].

The photodegradation of NBB dye was also evaluated using UV light without a photocatalyst, which aims to determine the effect of UV radiation through photolysis reactions. Under the same reaction conditions (initial concentration of NBB dye, pH, and radiation time), the utilization of UV light in the photolysis reaction of NBB dye for 270 minutes only resulted in a percent removal of NBB of 4.95% (Figure 9). Meanwhile, under the same photocatalytic reaction conditions for 270 minutes, ZnO nanoparticles could degrade nearly all NBB dyes (98.82%). These results indicate that the presence of ZnO

photocatalyst has a major effect on the photodegradation process of NBB dyes. This is because the photocatalytic reaction of ZnO with UV radiation can produce hydroxyl radicals ($\cdot\text{OH}$) and superoxide ions ($\text{O}_2^{\cdot-}$). These active species can damage the bonds in NBB dyes through a redox reaction, thereby transforming the NBB dyes from the initial blue into a clear color.

Furthermore, to confirm that the dye removal is indeed a photocatalytic process, an adsorption test under dark conditions was concurrently conducted alongside the photocatalytic reaction for 300 minutes. Under dark conditions for 300 minutes, ZnO nanoparticles can absorb 54.80% NBB dye. This shows the relatively high adsorption efficacy of ZnO on NBB dyes. This phenomenon can be attributed to the acidic conditions ($\text{pH} = 2$), wherein the surface of ZnO nanoparticles acquires a positive charge. Consequently, there is an increase in electrostatic attraction between the positively charged ZnO nanoparticles and the anionic NBB dye molecules, resulting in enhanced adsorption. The NBB dye molecules are thereby more readily adsorbed onto the surface of ZnO nanoparticles. When the dye solution (NBB) is acidic, $\text{pH} < \text{pH}_{\text{zpc}}$ (zero potential ZnO is around 8), the ZnO surface is positively charged, and the adsorption capacity of the NBB dye increases due to the electrostatic attraction of anionic NBB dye [36, 37].

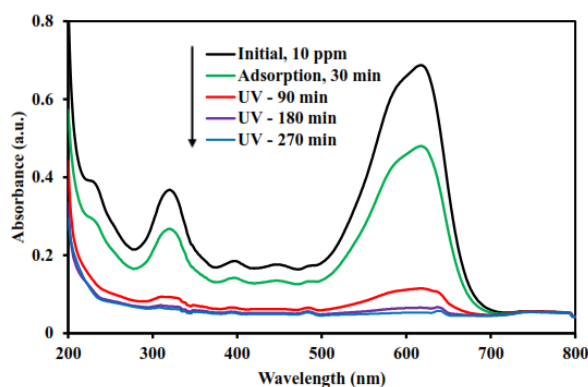


Figure 8. UV-Vis spectra of initial and after photodegradation of NBB dye solutions using ZnO nanoparticles at various irradiation times under UV light

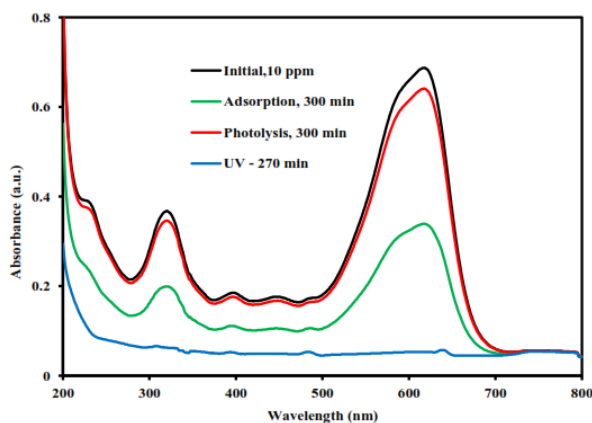


Figure 9. UV-Vis spectra of the initial NBB dye solution and after photodegradation using UV light (irradiation time 270 minutes) and dark condition (adsorption)

4. Conclusion

ZnO nanoparticles have been synthesized using a green method using water extract from red dragon fruit stems. The XRD data showed that synthesized ZnO NPs have a hexagonal zincite phase with an average crystallite size of 79.09 nm, confirming the ZnO nanostructure. The SEM-EDX analysis revealed that the ZnO nanoparticles exhibited a spherical morphology, displayed a uniform size distribution, and were evenly distributed. The evaluation of photocatalytic activity revealed that ZnO nanoparticles exhibit a notably high level of efficacy in facilitating the photodegradation process of NBB dye. ZnO nanoparticles exhibited an impressive capability to degrade NBB dye, achieving a remarkable 98.82% degradation after exposure to UV light for 270 minutes. This high photocatalytic activity of ZnO was attained under specific conditions: a pH value of 2 for the NBB solution, a photocatalyst dosage of 250 mg, and a NBB concentration of 10 ppm.

Acknowledgment

The authors gratefully acknowledge the financial support from the Ministry of Education, Culture, Research and Technology, Republic of Indonesia, through Universitas Syiah Kuala for the PTM Research Grant number 145/E5/PG.02.00.PT/2022.

References

- [1] Saad S. M. Hassan, Waleed I. M. El Azab, Hager R. Ali, Mona S. M. Mansour, Green synthesis and characterization of ZnO nanoparticles for photocatalytic degradation of anthracene, *Advances in Natural Sciences: Nanoscience and Nanotechnology*, 6, (2015), 045012 <https://doi.org/10.1088/2043-6262/6/4/045012>
- [2] Natheer B. Mahmood, Farqad R. Saeed, Kadhim R. Gbashi, Um-Salama Mahmood, Synthesis and characterization of zinc oxide nanoparticles via oxalate co-precipitation method, *Materials Letters: X*, 13, (2022), 100126 <https://doi.org/10.1016/j.mlblux.2022.100126>
- [3] Monika Patel, Sunita Mishra, Ruchi Verma, Deep Shikha, Synthesis of ZnO and CuO nanoparticles via Sol gel method and its characterization by using various technique, *Discover Materials*, 2, (2022), 1 <https://doi.org/10.1007/s43939-022-00022-6>
- [4] Vjaceslavs Gerbreders, Marina Krasovska, Eriks Sledevskis, Andrejs Gerbreders, Irena Mihailova, Edmunds Tamanis, Andrejs Ogurcovs, Hydrothermal synthesis of ZnO nanostructures with controllable morphology change, *CrystEngComm*, 22, 8, (2020), 1346-1358 <https://doi.org/10.1039/C9CE01556F>
- [5] S. Wirunchit, P. Gansa, W. Koetnuyom, Synthesis of ZnO nanoparticles by Ball-milling process for biological applications, *Materials Today: Proceedings*, 47, (2021), 3554-3559 <https://doi.org/10.1016/j.matpr.2021.03.559>
- [6] Wahyu Firmansya Nursalam, Lidya Irma Momuat, Henry Fonda Aritonang, Synthesis of Zinc Oxide (ZnO) Nanoparticles Using Microwave Assistance and Its Application as Photocatalyst in Degrading Methylene Blue, *Jurnal Kimia Sains dan Aplikasi*, 26, 1, (2023), 6 <https://doi.org/10.14710/jksa.26.1.28-33>
- [7] Shilpa Hiremath, C. Vidya, M. A. Lourdu Antonyraj, M. N. Chandraprabha, R. Srinidhi, R. Manjunath, Padanabha, Himanshu Agrawal, Photocatalytic degradation of Rhodamine B using Bio synthesized ZnO, *International Review of Applied Biotechnology and Biochemistry*, 2, 1, (2014), 207-213
- [8] Saeid Taghavi Fardood, Ali Ramazani, Sajjad Moradi, Pegah Azimzadeh Asiabi, Green synthesis of zinc oxide nanoparticles using arabic gum and photocatalytic degradation of direct blue 129 dye under visible light, *Journal of Materials Science: Materials in Electronics*, 28, (2017), 13596-13601 <https://doi.org/10.1007/s10854-017-7199-5>
- [9] Hirotaka Natori, Koichi Kobayashi, Masashi Takahashi, Preparation and Photocatalytic Property of Phosphorus-doped TiO₂ Particles, *Journal of Oleo Science*, 58, 7, (2009), 389-394 <https://doi.org/10.5650/jos.58.389>
- [10] Sreeshas Sasi, P. H. Fathima Fasna, T. K. Bindu Sharmila, C. S. Julie Chandra, Jolly V. Antony, Vidya Raman, Ajalesh B. Nair, Hareesh N. Ramanathan, Green synthesis of ZnO nanoparticles with enhanced photocatalytic and antibacterial activity, *Journal of Alloys and Compounds*, 924, (2022), 166431 <https://doi.org/10.1016/j.jallcom.2022.166431>
- [11] Vineet Kumar, Sudesh Kumar Yadav, Plant-mediated synthesis of silver and gold nanoparticles and their applications, *Journal of Chemical Technology & Biotechnology*, 84, 2, (2009), 151-157 <https://doi.org/10.1002/jctb.2023>
- [12] K. S. Mukunthan, S. Balaji, Cashew Apple Juice (*Anacardium occidentale* L.) Speeds Up the Synthesis of Silver Nanoparticles, *International Journal of Green Nanotechnology*, 4, 2, (2012), 71-79 <https://doi.org/10.1080/19430892.2012.676900>
- [13] Sachin, Jaishree, Nahar Singh, Rajni Singh, Kalpit Shah, Biplob Kumar Pramanik, Green synthesis of zinc oxide nanoparticles using lychee peel and its application in anti-bacterial properties and CR dye removal from wastewater, *Chemosphere*, 327, (2023), 138497 <https://doi.org/10.1016/j.chemosphere.2023.138497>
- [14] Shashanka Rajendrachari, Parham Taslimi, Abdullah Cahit Karaoglanli, Orhan Uzun, Emre Alp, Gururaj Kudur Jayaprakash, Photocatalytic degradation of Rhodamine B (RhB) dye in waste water and enzymatic inhibition study using cauliflower shaped ZnO nanoparticles synthesized by a novel One-pot green synthesis method, *Arabian Journal of Chemistry*, 14, 6, (2021), 103180 <https://doi.org/10.1016/j.arabjc.2021.103180>
- [15] Mohammad Aminuzzaman, Pei Sian Ng, Wee-Sheng Goh, Sayaka Ogawa, Akira Watanabe, Value-adding to dragon fruit (*Hylocereus polyrhizus*) peel biowaste: green synthesis of ZnO nanoparticles and their characterization, *Inorganic and Nano-Metal Chemistry*, 49, 11, (2019), 401-411 <https://doi.org/10.1080/24701556.2019.1661464>
- [16] B. Vishnupriya, G. R. Elakkiya Nandhini, G. Anbarasi, Biosynthesis of zinc oxide nanoparticles using *Hylocereus undatus* fruit peel extract against clinical pathogens, *Materials Today: Proceedings*, 48, (2022), 164-168 <https://doi.org/10.1016/j.matpr.2020.05.474>

- [17] Hamza Ferkous, Oualid Hamdaoui, Slimane Merouani, Sonochemical degradation of naphthol blue black in water: Effect of operating parameters, *Ultrasonics Sonochemistry*, 26, (2015), 40–47 <https://doi.org/10.1016/j.ultsonch.2015.03.013>
- [18] Ayça Atılır Özcan, Ali Özcan, Investigation of applicability of Electro-Fenton method for the mineralization of naphthol blue black in water, *Chemosphere*, 202, (2018), 618–625 <https://doi.org/10.1016/j.chemosphere.2018.03.125>
- [19] Indriaty Indriaty, Djufri Djufri, Binawati Ginting, Kartini Hasballah, Phytochemical screening, phenolic and flavonoid content, and antioxidant activity of Rhizophoraceae methanol extracts from Langsa, Aceh, Indonesia, *Biodiversitas Journal of Biological Diversity*, 24, 5, (2023), 2865–2876 <https://doi.org/10.13057/biodiv/d240541>
- [20] Erum Iqbal, Kamariah Abu Salim, Linda B. L. Lim, Phytochemical screening, total phenolics and antioxidant activities of bark and leaf extracts of *Goniothalamus velutinus* (Airy Shaw) from Brunei Darussalam, *Journal of King Saud University - Science*, 27, 3, (2015), 224–232 <https://doi.org/10.1016/j.jksus.2015.02.003>
- [21] Dineo A. Bopape, David E. Motaung, Nomso C. Hintsho-Mbita, Green synthesis of ZnO: Effect of plant concentration on the morphology, optical properties and photodegradation of dyes and antibiotics in wastewater, *Optik*, 251, (2022), 168459 <https://doi.org/10.1016/j.ijleo.2021.168459>
- [22] S. Lubis, M. Ramli, Sheilatina, Y. Ermanda, Hydrothermal Synthesis of Activated Carbon/ α - Fe₂O₃ Nanocomposite and Its Application for Removing Tartrazine Dye, *IOP Conference Series: Materials Science and Engineering*, 796, (2020), 012061 <https://doi.org/10.1088/1757-899X/796/1/012061>
- [23] Shayma Tahsin Karam, Ahmed Fattah Abdulrahman, Green Synthesis and Characterization of ZnO Nanoparticles by Using Thyme Plant Leaf Extract, *Photonics*, 9, 8, (2022), 594 <https://doi.org/10.3390/photonics9080594>
- [24] Azeez Abdullah Barzinjy, Himdad Hamad Azeez, Green synthesis and characterization of zinc oxide nanoparticles using *Eucalyptus globulus* Labill. leaf extract and zinc nitrate hexahydrate salt, *SN Applied Sciences*, 2, (2020), 991 <https://doi.org/10.1007/s42452-020-2813-1>
- [25] Zia-ur-Rehman Mashwani, Tariq Khan, Mubarak Ali Khan, Akhtar Nadhman, Synthesis in plants and plant extracts of silver nanoparticles with potent antimicrobial properties: current status and future prospects, *Applied Microbiology and Biotechnology*, 99, (2015), 9923–9934 <https://doi.org/10.1007/s00253-015-6987-1>
- [26] Yajing Huang, Choon Yian Haw, Ziyue Zheng, Junyong Kang, Jin-Cheng Zheng, Hui-Qiong Wang, Biosynthesis of Zinc Oxide Nanomaterials from Plant Extracts and Future Green Prospects: A Topical Review, *Advanced Sustainable Systems*, 5, 6, (2021), 2000266 <https://doi.org/10.1002/adsu.202000266>
- [27] R. Shashanka, Halil Esgin, Volkan Murat Yilmaz, Yasemin Caglar, Fabrication and characterization of green synthesized ZnO nanoparticle based dye-sensitized solar cells, *Journal of Science: Advanced Materials and Devices*, 5, 2, (2020), 185–191 <https://doi.org/10.1016/j.jsamd.2020.04.005>
- [28] Bushra H. Shnawa, Samir M. Hamad, Azeez A. Barzinjy, Payman A. Kareem, Mukhtar H. Ahmed, Scolicidal activity of biosynthesized zinc oxide nanoparticles by *Mentha longifolia* L. leaves against *Echinococcus granulosus* protoscolices, *Emergent Materials*, 5, (2022), 683–693 <https://doi.org/10.1007/s42247-021-00264-9>
- [29] Hao Cai, Dongshuo Zhang, Xiaolong Ma, Zichuan Ma, A novel ZnO/biochar composite catalysts for visible light degradation of metronidazole, *Separation and Purification Technology*, 288, (2022), 120633 <https://doi.org/10.1016/j.seppur.2022.120633>
- [30] M. S. Geetha, H. Nagabhushana, H. N. Shivananjai, Green mediated synthesis and characterization of ZnO nanoparticles using *Euphorbia* *Jatropha* latex as reducing agent, *Journal of Science: Advanced Materials and Devices*, 1, (2016), 301–310 <https://doi.org/10.1016/j.jsamd.2016.06.015>
- [31] S. Sheik Mydeen, R. Raj Kumar, M. Kottaisamy, V. S. Vasantha, Biosynthesis of ZnO nanoparticles through extract from *Prosopis juliflora* plant leaf: Antibacterial activities and a new approach by rust-induced photocatalysis, *Journal of Saudi Chemical Society*, 24, 5, (2020), 393–406 <https://doi.org/10.1016/j.jscs.2020.03.003>
- [32] Raunak Saha, Karthik Subramani, Saheri Sikdar, Kaniz Fatma, Suriyaprabha Rangaraj, Effects of processing parameters on green synthesised ZnO nanoparticles using stem extract of *Swertia chirayita*, *Biocatalysis and Agricultural Biotechnology*, 33, (2021), 101968 <https://doi.org/10.1016/j.bcab.2021.101968>
- [33] Meron Girma Demissie, Fedlu Kedir Sabir, Gemechu Deressa Edossa, Bedasa Abdisa Gonfa, Synthesis of Zinc Oxide Nanoparticles Using Leaf Extract of *Lippia adoensis* (Koseret) and Evaluation of Its Antibacterial Activity, *Journal of Chemistry*, 2020, (2020), 7459042 <https://doi.org/10.1155/2020/7459042>
- [34] Mahmoud Nabil, I. V. Perez-Quintana, M. Acosta, J. A. Mendez-Gamboa, R. Castro-Rodriguez, Morphological, Structural, and Optical Bandgap Characterization of Extracted ZnO Nanoparticles from Commercial Paste, *Advances in Materials Science and Engineering*, 2021, (2021), 9926544 <https://doi.org/10.1155/2021/9926544>
- [35] Gcina Mamba, Xavier Yangkou Mbianda, Ajay Kumar Mishra, Photocatalytic degradation of the diazo dye naphthol blue black in water using MWCNT/Gd,N,S-TiO₂ nanocomposites under simulated solar light, *Journal of Environmental Sciences*, 33, (2015), 219–228 <https://doi.org/10.1016/j.jes.2014.06.052>
- [36] Shanhong Lan, Hao Zhang, Junjie Hu, Shiwen Geng, Huixia Lan, Effects of pH value on photocatalytic performance of ZnO composite graphene for degradation of methyl orange, *Journal of Optoelectronics and Advanced Materials*, 20, May–June 2018, (2018), 337–345 <https://doi.org/10.1007/s10854-016-5660-5>
- [37] Theepakorn Sansenya, Nataporn Masri, Tammanoon Chankhanittha, Teeradech Senasu, Jirayus Piriyanon, Siriboon Mukdasai, Suwat Nanan, Hydrothermal synthesis of ZnO photocatalyst for detoxification of anionic azo dyes and antibiotic,

Journal of Physics and Chemistry of Solids, 160, (2022),
110353 <https://doi.org/10.1016/j.jpics.2021.110353>